



AdvFAS: a robust face anti-spoofing framework against adversarial examples

Jiawei Chen^a, Xiao Yang^b, Heng Yin^a, Mingzhi Ma^a, Bihui Chen^d, Jianteng Peng^d, Yandong Guo^d, Zhaoxia Yin^e, Hang Su^{b,c}

^aAnhui Provincial Key Laboratory of Multimodal Cognitive Computation, Anhui University, Hefei 230601, China.

^bDepartment of Computer Science and Technology, Institute for AI, THBI Lab, Tsinghua University, Beijing 100084, China.

^cZhongguancun Laboratory, Beijing, 100080, China

^dOPPO Research Institute, Beijing, China

^eShanghai Key Laboratory of Multidimensional Information Processing, East China Normal University, Shanghai 200241, China.

ABSTRACT

Ensuring the reliability of face recognition systems against presentation attacks necessitates the deployment of face anti-spoofing techniques. Despite considerable advancements in this domain, the ability of even the most state-of-the-art methods to defend against adversarial examples remains elusive. While several adversarial defense strategies have been proposed, they typically suffer from constrained practicability due to inevitable trade-offs between universality, effectiveness, and efficiency. To overcome these challenges, we thoroughly delve into the coupled relationship between adversarial detection and face anti-spoofing. Based on this, we propose a robust face anti-spoofing framework, namely AdvFAS, that leverages two coupled scores to accurately distinguish between correctly detected and wrongly detected face images. Extensive experiments demonstrate the effectiveness of our framework in a variety of settings, including different attacks, datasets, and backbones, meanwhile enjoying high accuracy on clean examples. Moreover, we successfully apply the proposed method to detect real-world adversarial examples.

© 2023 Elsevier Ltd. All rights reserved.

1. Introduction

The proliferation of face recognition systems has underscored the paramount importance of face anti-spoofing technology (Yang et al., 2014; Wang et al., 2022c; Yu et al., 2022, 2021; Yang et al., 2019). This technology aims to distinguish between real human faces and various presentation attacks (face substitutes), such as print, video replay, 3D mask attacks, *etc.* As highlighted by (Szegedy et al., 2013), deep neural networks are vulnerable to adversarial examples, which incorporate concealed messages into images. Furthermore, face recognition systems (Yang et al., 2021a; Yin et al., 2021; Yang et al., 2021b) based on deep neural networks also have exhibited their vulnerability against adversarial examples. In terms of face anti-spoofing, adversarial examples can fool face anti-spoofing systems by introducing adversarial perturbations to the face substitutes, resulting in the paralysis of face recognition systems. Therefore, the creation of more realistic spoofing faces while

encompassing a wide range of attack types remains a pressing concern in the domain of presentation attacks.

Moreover, the study of adversarial attacks is crucial to maximize the effect of presentation attacks¹, where the breadth of attacks is a pivotal consideration. Adversarial attacks can be superimposed on existing face substitutes, endowing more examples with the ability to deceive face anti-spoofing technology.

Therefore, in security-sensitive applications, face anti-spoofing must exhibit enough robustness against both presentation attacks and adversarial attacks.

However, few studies have been concerned about defending adversarial examples in face anti-spoofing. (Bousnina et al., 2021) propose to defend differential evolution-based adversarial attacks using eight data augmentation techniques, which only concern the specific attack. UniFAD (Deb et al., 2021) is proposed in an attempt to merge digital attacks and presentation attacks under one framework. However, UniFAD requires a large number of images to be prepared in advance to train an

**Corresponding author
e-mail: suhangss@mail.tsinghua.edu.cn (Hang Su)

¹We do not consider real-to-fake attacks because they pose an ill-suited threat to face recognition systems

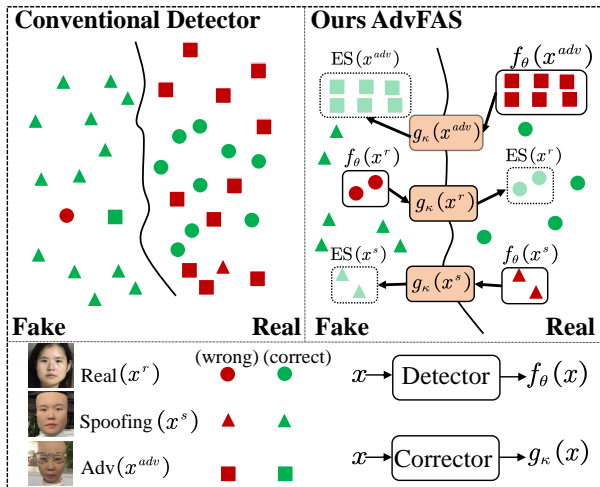


Fig. 1. Left: Conventional detector methods demonstrate very poor performance in defending adversarial examples. Right: Our AdvFAS can distinguish wrongly detected examples from correctly detected ones through two coupled scores: $f_\theta(x)$ and $ES(x)$. $ES(x)$ refers to the expected score. $g_\kappa(x)$ builds the bridge between $f_\theta(x)$ and $ES(x)$.

additional network. Another limitation is that both of them focus on detecting black-box attacks, which ignore the more challenging white-box attack detection. Compared to black-box attacks, it can only observe the output of the targeted model. An attacker has complete access to the target model in white-box settings, including the architecture and parameters of the model. Since black-box attacks are a more realistic assumption in the real world, evaluating models against white-box attacks is crucial to measure the performance of the model in the worst-case scenarios (Wiyatno et al.). Moreover, defenses against white-box attacks resist insiders, who could access the model by maliciously creating adversarial examples to jeopardize the performance of face recognition systems.

Adversarial training is recognized as an effective approach to defending against white-box attacks (Madry et al., 2017; Zhang et al., 2019). However, this approach typically leads to degraded detection performance on clean examples. This phenomenon is unacceptable in face anti-spoofing. A recent work (Pang et al., 2022) proposes that adversarial examples could be provably told apart by two coupled rejection metrics. This approach performs excellently against white-box adversarial attacks and is compatible with different models for improving robustness. It inspired us to explore the coupled relationship between face anti-spoofing and adversarial detection.

In this paper, we explore the coupled relationship between the two tasks, as illustrated in Fig. 1, and propose a novel robust framework (AdvFAS) for face anti-spoofing to detect white-box adversarial examples. In Sec. 3.2, we present the theoretical analysis of this coupled relationship in detecting adversarial examples. Specifically, two coupled scores, $f_\theta(x)$ and $ES(x)$, are defined to explicitly represent the coupled relationship. $f_\theta(x)$ is the output score of the conventional detector, and $ES(x)$ is the expected score. In the case of correctly detected examples, $ES(x)$ is equal to $f_\theta(x)$. $ES(x)$ is equal to the ground truth label (0 or 1) for wrongly detected examples. However, due to

the absence of the true label y , we are unable to obtain $ES(x)$ during testing. Therefore, a correction score $g_\kappa(x)$ is introduced to assist to predict $ES(x)$. We realize that the conventional detector structure is not sufficient to solve this problem with a single score $f_\theta(x)$, *i.e.*, an additional structure (named corrector) is required to calculate $g_\kappa(x)$. To save memory costs, we adopt a shared block with a two-head structure to model the detector and the corrector. The accuracy of clean examples is vulnerable to over-involvement of the adversarial examples during training. Thus, some strategies (such as stopping gradients and adding a mask) are adopted to eliminate the negative effects, which are illustrated in detail in Sec. 3.3.

To demonstrate the effectiveness of the framework, we conduct experiments on three widely used backbones (Depthnet (Liu et al., 2018), Resnet-18 (He et al., 2016), and Resnet-50), two publicly available datasets (WMCA (George et al., 2019) and CASIA-SURF 3DMask (Yu et al., 2020)), and two adversarial attack methods (PGD (Madry et al., 2017) and patch attack (Tong et al., 2021)). In addition, we apply the proposed framework to CMFL (George and Marcel, 2021a) to verify its effectiveness on multi-modal inputs.

Extensive experiments demonstrate that the proposed framework is suitable for various scenarios and obtains state-of-the-art performance. Moreover, adaptive attacks (Tramer et al., 2020) are designed to evade our corrector module, for the purpose of fully validating the effectiveness of the proposed framework. We further apply our framework to detect real-world adversarial examples, in order to show its practical applicability.

Our main contributions are summarized as follows:

- We thoroughly explore the coupled relationship between face anti-spoofing and adversarial detection and propose a novel face anti-spoofing framework against adversarial examples.
- We present a theoretical analysis that two coupled scores can distinguish wrongly detected face images from correctly detected ones.
- Extensive experiments show that the proposed framework is universal and effective in various scenarios. The highest accuracy on adversarial examples increased by 93.79%.

2. Related Work

Face Anti-Spoofing. There has been increasing research on face anti-spoofing in the last decade (Yu et al., 2022). During the first few years, traditional handcrafted features (Pan et al., 2007; Li et al., 2016; Freitas Pereira et al., 2012; Komulainen et al., 2013; Patel et al., 2016) were utilized to detect print attacks. These include liveness cues, eye-blinking (Pan et al., 2007; Jee et al., 2006; Li, 2008), head, face motion, and gaze tracking. However, these handcrafted features cannot be elegantly applied because they require rich prior knowledge and are vulnerable to being fooled by attacks with dynamic characteristics (*eg*, replay attacks). With the development of deep learning, many researchers have turned to deep learning to achieve face anti-spoofing. Some research (Zhang et al., 2021;

Li et al., 2021; Ming et al., 2022) focuses on using the whole RGB image to extract features. As illustrated by (Wang et al., 2022a; Grinchuk et al., 2021a), the network sometimes loses local information when training with whole faces. These approaches crop the face images into patches, trying to capture more local information. As presentation attacks become more realistic, RGB images of real faces and face substitutes become more difficult to distinguish. (George and Marcel, 2021b; Jia et al., 2021a; Wang et al., 2022b) utilize multi-modal information (eg, deep and infrared) or other sensors. These methods impose additional demands on sensors or deep estimation methods. Some studies (Jia et al., 2020, 2021a; Liu et al., 2022) demonstrated that the generalizability of the face anti-spoofing models is poor. These studies mainly investigate generalization to unseen domains and unknown attack types. In general, the research on face anti-spoofing tends to be diverse and practical. However, most face anti-spoofing research ignores the threat to face recognition systems from adversarial attacks.

Adversarial Examples Defense. The methods of defending against adversarial examples can be broadly categorized into two categories: adversarial training (Madry et al., 2017; Zhang et al., 2019; Wu et al., 2020) and adversarial detection (Metzen et al., 2017; Gong et al., 2017; Carrara et al., 2018; Zhang et al., 2018; Ma et al., 2018; Feinman et al., 2017). On the one hand, adversarial training is widely accepted as the most effective method to improve the adversarial robustness of deep learning models (Yu et al., 2022). The main idea is to make the network robust by adding adversarial examples to the training process through a min-max formulation. (Madry et al., 2017) proposed the PGD-AT, which significantly increased the adversarial robustness of deep learning models against a wide range of attacks. Based on PGD-AT, some derivative work has followed their designs and proposed settings such as AWP (Wu et al., 2020), TRADES (Zhang et al., 2019), and Free-AT (Shafahi et al., 2019), etc. However, adversarial training generally reduces the detection accuracy on clean examples (Madry et al., 2017), which is particularly evident in face anti-spoofing according to our experiments. On the other hand, adversarial detection bypasses the impact on the accuracy on clean examples by training an additional detector (Metzen et al., 2017; Gong et al., 2017; Carrara et al., 2018; Zhang et al., 2018) or designing statistics (Ma et al., 2018; Feinman et al., 2017). The pipeline of (Deb et al., 2021) is similar to adversarial detection. But training an additional network increases consumption, and the defense system will be destroyed when this network is attacked.

Due to such open challenges, we propose a novel robust face anti-spoofing framework against adversarial examples (Adv-FAS). Specifically, we find a coupled relationship between adversarial detection and face anti-spoofing, and use this relationship to merge the two tasks into a single framework.

3. Method

We propose a new robust framework for face anti-spoofing to detect adversarial examples by a corrector to correct the score of face anti-spoofing models, as illustrated in Fig. 2. Specifically,

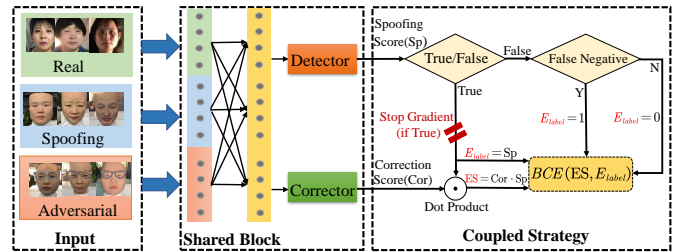


Fig. 2. Construction of the objective \mathcal{L}_{cor} in Eq. (7) for training the corrector, which is the binary cross-entropy (BCE) loss between $ES(x)$ and E_{label} . The corrector shares a main backbone with the detector, introducing little extra memory cost.

a two-head structure is adopted to implement the framework. One is a detector that does the conventional face anti-spoofing task; the other is a corrector that corrects the errors of the detector through a correction score. The combination of the two can be used to calculate an expected score as the final score for judging whether a face is real. In this section, we discuss the proposed framework in detail.

3.1. Problem Formulation

Defending against white-box adversarial attacks can always be formulated as a min-max problem and has also been verified to be effective. For a standard face anti-spoofing network (detector) f_θ , consider a data pair (x, y) , with $x \in \mathbb{R}^d$ as the input and y as the true label. Generally, the problem is formulated as a saddle point problem as follows:

$$\min_{\theta} \mathbb{E}_{p(x,y)} \left[\max_{\xi \in \mathcal{E}} \mathcal{L}(f_\theta(x + \xi), y) \right], \quad (1)$$

where the $x + \xi$ is the adversarial example generated by adding the perturbation ξ from set $\mathcal{E} = \{\xi : \|\xi\| \leq \epsilon\}$ to the clean example x . In this paper, the coupled relationship of the two tasks can be similarly formulated as a min-max problem.

What to Correct? Some previous approaches for adversarial examples detection have associated adversarial characters with error detection. However, face anti-spoofing for clean examples still has a few errors despite impressive detection. And, for adversarially trained face anti-spoofing models, there are still many adversarial examples that can be correctly detected. Therefore, in contrast to adversarial-based correction, it would be more reasonable to correct output based on whether the $f_\theta(x)$ will be wrong.

Couple Detector and Corrector. The problem scenario is that the detector has excellent performance on clean examples with few errors, but has poor ability to detect adversarial examples. This inspires us not to wholly overturn current face anti-spoofing technologies but to correct some of the $f_\theta(x)$. Therefore, the corrector is created to tackle the problem and we construct the expected score (ES) as:

$$ES(x) = f_\theta(x) \cdot g_\kappa(x), \quad (2)$$

where $g_\kappa(x) \in [0, 1]$ is the corrector output and parameterized

by κ . Through the ES, we expect the corrector to be aware of whether or not the $f_\theta(x)$ is correct and to correct the $f_\theta(x)$ when it is wrong. In other words, the ES, instead of $f_\theta(x)$, is treated as the final decision. In addition, the corrector and the detector are coupled: for a wrong $f_\theta(x)$, if the $f_\theta(x)$ is close to 1, the ES(x) must be close to 0 if the ES works (and vice versa). Because of this property, attackers cannot achieve successful attacks by attacking the detector or the corrector.

Optimization Goal. Assume that clean and adversarial examples are detected incorrectly as x'_c and x'_a respectively, where $x'_a = \arg \max_{x' \in S(x)} \mathcal{L}_{spoofer}(x', y; \theta)$. $S(x)$ is a set of allowed points around x (e.g., a ball of $\|x' - x\|_p \leq \epsilon$) and x is spoofing. $\mathcal{L}_{spoofer}$ means the loss of the detector. Suppose $x^* \in \{x'_c, x'_a\}$ is the input that is detected wrongly by the detector. The problem is formulated as:

$$\min_{\theta, \kappa} \mathbb{E}_{p(x, y)} \left[\mathcal{L}_{spoofer}(x, y; \theta) + \mathcal{L}_{cor}(x^*, y; \theta, \kappa) \right], \quad (3)$$

where the \mathcal{L}_{cor} is utilized to optimize ES. Moreover, $f_\theta(x)$ and $g_\kappa(x)$ conform in distribution to the above coupled property by concurrently optimizing θ and κ . Eq. (3) can be considered a min-max problem. For the inner maximization step, the most aggressive perturbation is found for the face anti-spoofing network under the ℓ_p norm constraint to generate adversarial examples, x'_a . The outer minimization objective is to detect clean examples correctly and to correct the wrongly detected examples. More details are given in Sec. 3.2 and Sec. 3.3.

3.2. Theoretical Analysis

The problem can be summarized into a set of cases C . C denotes all possible results for which the input x is detected by the detector. It can be split into FP : $\{x|x = spoofing|adv, x \in \mathbb{R}^d, f_\theta(x) \geq \frac{1}{2}\}$, FN : $\{x|x = real, x \in \mathbb{R}^d, f_\theta(x) < \frac{1}{2}\}$, TN : $\{x|x = spoofing|adv, x \in \mathbb{R}^d, f_\theta(x) < \frac{1}{2}\}$, and TP : $\{x|x = real, x \in \mathbb{R}^d, f_\theta(x) \geq \frac{1}{2}\}$. Where adv are generated from spoofing faces. Clearly, FP and FN are the wrong cases, while TN and TP are the correct cases.

At training time, we optimize ES by minimizing the binary cross-entropy (BCE) loss. Due to the diversity of cases and different optimization strategies of ES for different cases, an adaptive loss \mathcal{L}_{cor} was designed:

$$FP : \mathcal{L}_{cor}(x; \theta, \kappa) = BCE(f_\theta(x) \cdot g_\kappa(x), 0), \quad (4)$$

$$FN : \mathcal{L}_{cor}(x; \theta, \kappa) = BCE(f_\theta(x) \cdot g_\kappa(x), 1), \quad (5)$$

$$TN||TP : \mathcal{L}_{cor}(x; \theta, \kappa) = BCE(f_\theta(x) \cdot g_\kappa(x), f_\theta(x)). \quad (6)$$

Defining $E_{label} \in \{0, 1, f_\theta(x)\}$, the adaptive loss can thereby be rewritten as:

$$\mathcal{L}_{cor}(x; \theta, \kappa) = BCE(f_\theta(x) \cdot g_\kappa(x), E_{label}). \quad (7)$$

In this case, the optimal solution of minimizing \mathcal{L}_{cor} is $g_\kappa^*(x) = \frac{E_{label}}{f_\theta(x)}$. The corrector and the detector can be jointly optimized by minimizing:

Algorithm 1 the optimization strategy of AdvFAS

Input:A detector f_θ with loss function $\mathcal{L}_{spoofer}$ and a corrector g_κ with a coupled loss \mathcal{L}_{cor} .

Input:A clean example x and ground-truth label y (spoofing: 0, real: 1) and epochs E .

Output: $f_\theta(x)$, $g_\kappa(x)$.

```

1: for e = 0 to E-1 do
2:   if y = 0 then
3:     Generate perturbation  $\xi$  to  $x$ ;
4:      $x^* = x + \xi$ ;
5:   end if
6:   Put  $x$  to the detector  $f_\theta$ ;
7:   Put  $x$  and  $x^*$  to the corrector  $g_\kappa$ ;
8:   Minimize the  $\mathcal{L}_{spoofer}$ ;
9:   if  $f_\theta(x)$  or  $f_\theta(x^*)$  is correct then
10:    Stop the gradient of  $f_\theta(x)$  or  $f_\theta(x^*)$ ;
11:   end if
12:   Minimize the  $\mathcal{L}_{cor}$ .
13: end for
```

$$\mathcal{L}_{cs} = \mathcal{L}_{spoofer}(x; \theta) + \lambda \cdot \mathcal{L}_{cor}(x^*; \theta, \kappa). \quad (8)$$

Here, λ is a hyper-parameter that defaults to 1.0. The Eq. (8) has the same optimization objective as Eq. (3). In the training phase, the network simultaneously optimizes parameters for the detector and the corrector by \mathcal{L}_{cs} . The whole process is described in detail in Algorithm 1.

3.2.1. Theoretically Coupling ES and f_θ

Based on the above design of \mathcal{L}_{cor} , we state the optimization objectives of ES on different cases respectively. We observe that properly coupling f_θ and ES can provably separate wrongly and correctly detected inputs, as stated below:

Lemma 1. (Separability) Given the detector f_θ , $\forall x_1, x_2$ with spoofing scores larger than $\frac{1}{2}$, i.e.,

$$f_\theta(x_1) \geq \frac{1}{2}, \text{ and } f_\theta(x_2) \geq \frac{1}{2}. \quad (9)$$

If x_1 is detected correctly, while x_2 is detected wrongly, then $ES(x_1) > \frac{1}{2} > ES(x_2)$.

Proof. x_1 conforms to Eq. (6) because it is correctly detected, thus the $ES(x_1) = f_\theta(x_1) \geq \frac{1}{2}$. On the other side, x_2 is wrongly detected and $f_\theta(x_2) \geq \frac{1}{2}$, so it conforms to Eq. (4) and we have $ES(x_2) = 0 < \frac{1}{2}$. As for other cases, we have a similar conclusion.

Lemma 2. (Separability) Given the detector f_θ , $\forall x_1, x_2$ with spoofing scores less than $\frac{1}{2}$, i.e.,

$$f_\theta(x_1) < \frac{1}{2}, \text{ and } f_\theta(x_2) < \frac{1}{2}. \quad (10)$$

If x_1 is detected correctly, while x_2 is detected wrongly, then $ES(x_1) < \frac{1}{2} < ES(x_2)$.

Proof. x_1 conforms to Eq. (6) because it is correctly detected, thus the $ES(x_1) = f_\theta(x_1) < \frac{1}{2}$. On the other side, x_2 is wrongly detected and $f_\theta(x_2) < \frac{1}{2}$, so it conforms to Eq. (5) and we have $ES(x_2) = 1 \geq \frac{1}{2}$.

According to Lemma 1 (Lemma 2), when the spoofing scores of the detector are larger (less) than $\frac{1}{2}$, then for any x that passes the detector, $ES(x) \geq \frac{1}{2}$ ($ES(x) < \frac{1}{2}$) as long as x is correctly detected; conversely, $ES(x) < \frac{1}{2}$ ($ES(x) \geq \frac{1}{2}$). The property of the two coupled scores can be utilized to distinguish wrongly detected examples from correctly detected ones.

3.2.2. Coupling in Practice ES and f_θ

Sec. 3.2.1 shows that coupling ES and f_θ is properly separable for wrongly and correctly detected inputs. However, during actual training, there is necessarily an error between $g_\kappa(x)$ and $g_\kappa^*(x)$. We introduce a definition on the point-wise error between $g_\kappa(x)$ and $g_\kappa^*(x)$:

Definition 1. (Point-wisely δ -error). If a point x satisfies the following range:

$$|g_\kappa(x) - g_\kappa^*(x)| \leq \frac{\delta}{2}, \quad (11)$$

where $\delta \in [0, 1)$, then g_κ is called δ -error at the input x .

For any $g_\kappa(x)$ trained to be better than a random guess at x , the δ is always found to satisfy Definition 1. In particular, assume that $g_\kappa(x)$ performs a random guess on x , meaning $g_\kappa(x) = \frac{1}{2}$. Because $g_\kappa^*(x) \in [0, 1]$, there is $|\frac{1}{2} - g_\kappa^*(x)| \leq \frac{1}{2}$, which means that even a random guess $g_\kappa(x)$ can satisfy Definition 1 with $\delta = 1$.

We prove the separability of wrongly and correctly detected inputs at the optimal threshold equal to $\frac{1}{2}$ in Lemma 1. However, in practice we cannot access the optimal threshold, which is not always equal to $\frac{1}{2}$ due to training error. To this end, we demonstrate that the detector with $\frac{1}{2-\delta}$ and the corrector with δ -error $g_\kappa(x)$ can be coupled to achieve separability, similarly to the property shown in Lemma 1.

Theorem 1. (Separability) Given the detector f_θ , for any x_1, x_2 with spoofing scores larger than $\frac{1}{2-\delta}$, i.e.,

$$f_\theta(x_1) > \frac{1}{2-\delta}, \text{ and } f_\theta(x_2) > \frac{1}{2-\delta}, \quad (12)$$

where $\delta \in [0, 1)$, x_1 and x_2 are detected correctly and wrongly respectively, and g_κ is δ -error at x_1, x_2 , then there must be $ES(x_1) > \frac{1}{2} > ES(x_2)$.

Specifically, after we reset the threshold of the corrector to $\frac{1}{2-\delta}$ and obtain the remaining examples, any wrongly detected examples will be corrected correctly by the ES, as long as g_κ is trained to be δ -error for these examples.

Proof. The conditions in Theorem 1 can be written as x_1 is correctly detected, $f_\theta(x_1) > \frac{1}{2-\delta}$ and x_2 is wrongly detected, $f_\theta(x_2) > \frac{1}{2-\delta}$, where $\delta \in [0, 1)$. Since $g_\kappa(x)$ is δ -error at x_1 and x_2 , according to Definition 1, we have the following range:

$$|g_\kappa(x) - g_\kappa^*(x)| \leq \frac{\delta}{2}. \quad (13)$$

For x_1 , there is $g_\kappa^*(x_1) = 1$. And we can obtain

$$\begin{aligned} ES(x_1) &= f_\theta(x_1) \cdot g_\alpha(x_1) > f_\theta(x_1) \cdot \left(\frac{2-\delta}{2}\right) \\ &> \left(\frac{1}{2-\delta}\right) \cdot \left(\frac{2-\delta}{2}\right) = \frac{1}{2}. \end{aligned} \quad (14)$$

Similarly for x_2 , there is $g_\kappa^*(x_2) = 0$. We can obtain:

$$\begin{aligned} ES(x_2) &= f_\theta(x_2) \cdot g_\alpha(x_2) < f_\theta(x_2) \cdot \frac{\delta}{2} \\ &< \frac{1}{2-\delta} \cdot \frac{\delta}{2} < \frac{1}{2}. \end{aligned} \quad (15)$$

Thus we have proven $ES(x_1) > \frac{1}{2} > ES(x_2)$ and the Theorem 1 is established.

3.3. Framework Details

Coupling Loss Design. The \mathcal{L}_{cs} consists of \mathcal{L}_{spooof} and \mathcal{L}_{cor} . The former is the same as the conventional face anti-spoofing methods and the latter is utilized to optimize the corrector. Therefore, the conventional loss of face anti-spoofing is not altered during training. In other words, the model degenerates to the regular face anti-spoofing model when λ is equal to 0. The particularity ensures that the proposed framework is compatible with different face anti-spoofing frameworks. (In the case of the loss function, it is sufficient to add \mathcal{L}_{cor}).

Shared Block. There are three types of possible inputs: adversarial examples generated from spoofing faces, spoofing faces, and real faces. During the training period, all three types of images are shuffled and then input into the shared block. The shared block simultaneously optimizes parameters for the detector and the corrector. Compared to training on an additional network, the design of a shared block saves computation and memory costs.

Stop Gradients and Add a Mask. When the images are detected correctly, stopping gradients on the spoof scores of \mathcal{L}_{cor} can avoid focusing on easy examples and keep the optimal solution of the detector unbiased. In particular, we use $p(x, y)$ to represent data distribution. For \mathcal{L}_{spooof} , the optimal solution of minimizing $\mathcal{L}_{spooof}(f_\theta(x), y)$ is $f_\theta(x)[y] = p(y|x)$. However, if we do not stop gradients of $f_\theta(x)[y]$ in the corrector, then the optimal θ of the entire framework objective no longer satisfies $f_\theta(x)[y] = p(y|x)$. In this case, the corrector will introduce bias in the optimal solution of the detector. A mask is utilized to eliminate the loss of adversarial examples to ensure that the corrector works as conventionally as possible during training. Specifically, the mask, which is an image-level (0, 1) matrix, is implemented to separate adversarial examples from clean examples (real and spoofing). The zeros in the matrix correspond to the adversarial examples. For a mask $\mathcal{M} = \{m_i\}_{i=1}^n$, where n represents the number of images and $m_i \in \{0, 1\}$ refers to the i -th image. Define x_i as i -th examples. We can formulate as:

$$\mathcal{L}_{spooof}(x_i, \theta) = m_i \cdot L_{spooof}(x_i, \theta). \quad (16)$$

Without the mask, there may be problems caused by data imbalance. During the training time, too much participation of the adversarial examples will affect the detection of clean examples.

4. Experiments

4.1. Experimental Settings

Data Preparation. The WMCA and CASIA-SURF 3DMask are used in our experiments as evaluation datasets. WMCA is a publicly available face image dataset that contains a variety of presentation attacks in 2D and 3D, such as paper print, video replay, and 3D mask. We use the grandtest protocol of WMCA to divide it into the training set, validation set, and test set. Compared with WMCA, face data on CASIA-SURF 3DMask is in video format. Therefore, data pre-processing is required for the CASIA-SURF 3DMask. To obtain this, we extract one frame out of every three frames of each video and adopt MTCNN(Zhang et al., 2016) for face detection. Then, we crop and resize each extracted frame to the size of 128×128 . Finally, we utilize an appropriate proportion to divide these pre-processing frames into the training set, the validation set, and the test set.

Network Setting. The detector and corrector of the two-head structure adopt the same neural network, such as Depthnet, Resnet-18, and Resnet-50. Moreover, deep pixel-wise binary supervision (George and Marcel, 2019) is utilized to improve the performance of these neural networks for face anti-spoofing.

Attack Setting. Five publicly available adversarial attacks are used in our experiments, including C&W(Carlini and Wagner, 2017), PGD, patch attack, DeepFool(Moosavi-Dezfooli et al., 2016) and AutoAttack(Croce and Hein, 2020). C&W, PGD, AutoAttack, and DeepFool are the most popular and powerful adversarial attacks in the digital world. In contrast, patch attack is easily realized in the physical world and has excellent attack capability.

Training Setting. The batch size is set to 100. The \mathcal{L}_{cs} is optimized with the $\lambda=1.0$. An Adam optimizer with a learning rate (lr) of $1e-3$ and a weight decay of $5e-5$ is applied to our experiments. We first base testing on a validation set to measure the optimal threshold. Then, the optimal threshold is utilized to calculate the final detection score on a test set.

Table 1. The success rates (%) of adversarial attacks against three models we study. The adversarial examples are crafted for HRFP, CMFL and DBMnet respectively using C&W, PGD, patch, DeepFool and AutoAttack on WMCA and CASIA-SURF 3DMask.

Method	WMCA			CASIA-SURF 3DMask		
	HRFP	CMFL	DBMnet	HRFP	CMFL	DBMnet
C&W	90.10	100.0	100.0	71.80	100.0	100.0
PGD	87.40	97.55	100.0	80.00	99.82	99.65
Patch	81.21	86.86	100.0	73.60	98.10	100.0
DeepFool	90.00	100.0	100.0	74.20	100.0	100.0
AutoAttack	97.00	100.0	99.78	88.40	100.0	99.78



Fig. 3. The adversarial examples are crafted on WMCA and CASIA-SURF 3DMask by patch attack.

4.2. Vulnerability Evaluation of Existing Detectors

To evaluate the vulnerability of existing SOTA face-spoofing methods, High Resolution Face Parts (HRFP)(Grinchuk et al., 2021b), CMFL, and DBMnet (Jia et al., 2021b). are tested in adversarial attacks. HRFP achieved first place in the 3D High-Fidelity Mask Face Presentation Attack Detection Challenge based on the CASIA-SURF HiFiMask(Liu et al., 2021). To ensure fairness, the checkpoint shared by the original authors is adopted in the evaluation.

As shown in Tab. 1, we utilize adversarial attacks against these three methods mentioned above on WMCA and CASIA-SURF 3DMask respectively. Any success rate of adversarial attacks can simply be above 70%, which shows that existing face-spoofing methods are vulnerable to adversarial attacks. Especially under the attack configuration of C&W, DeepFool, PGD and AutoAttack in CMFL and DBMnet, success rates of adversarial attacks can approach 100% no matter on WMCA or CASIA-SURF 3DMask. Although HRFP segments each face data into different face features as input to a corresponding convolution network, success rates of adversarial attacks also reach above 80% on WMCA and 70% on CASIA-SURF 3DMask. Hence, the existing high-performance face-spoofing detectors can be easily broken by existing adversarial attack technologies, *i.e.*, it is necessary for face anti-spoofing methods to defend against adversarial examples.

4.3. Performance Against Different Settings

AdvFAS vs. PGD. The performance of the proposed framework and baselines against PGD in the grandtest protocol of WMCA are shown in Tab. 2, Tab. 3 and Tab. 6. In order to fully evaluate, we also use the AUC to evaluate our method and the baseline in Tab. 4. We test baselines and AdvFAS on four models: depthnet, resnet18, resnet50 and CMFL. For CMFL, we use the four channels of RGBD on WMCA. To provide a comprehensive comparison, we also conduct a comparison with FAS-wrapper(Guo et al., 2022) and Patchnet(Wang et al., 2022a). Due to their poor robustness, when training with clean examples, they have no ability to distinguish between adversarial examples and clean examples, although it has nice accuracy on the clean examples. The accuracy on adversarial examples is only around 20%. On the contrary, PGD-AT and PGD-AWP can recognize adversarial examples with higher accuracy, but these methods push the classification boundary of the training

Table 2. Performance of the baseline systems and the proposed framework against PGD on WMCA. The performance is tested on three models Depthnet, Resnet18, and Resnet50 respectively. Note that only color channels are used on WMCA. The ACC (w/o adv) (%) represents the accuracy of models in detecting clean examples. The ACC (adv) (%) is the accuracy of models in detecting adversarial examples. The ACC(adv) refers to the average test accuracy on clean and adversarial examples.

Method	Depthnet			Resnet18			Resnet50		
	ACC(w/o adv)	ACC(adv)	ACC(avg)	ACC(w/o adv)	ACC(adv)	ACC(avg)	ACC(w/o adv)	ACC(adv)	ACC(avg)
Clean	91.10	22.15	56.63	87.58	5.59	46.59	89.90	20.33	55.12
PGD-AT(eps=16/255)	25.43	99.87	62.65	22.25	100.0	61.13	25.07	94.69	59.88
PGD-AWP(eps=16/255)	34.94	78.68	56.81	29.31	95.84	62.58	22.14	100.0	61.07
PGD-AT(eps=8/255)	22.29	100.0	61.15	27.4	90.23	58.82	20.99	99.94	60.47
PGD-AWP(eps=8/255)	24.00	98.20	66.10	79.27	97.26	88.27	30.06	100.0	65.03
Ours	87.32	92.01	89.67	90.26	98.03	94.15	88.55	97.80	93.18

Table 3. Performance of the baseline systems and the proposed framework against PGD on WMCA. The performance is tested on CMFL.

Method	CMFL		
	ACC(w/o adv)	ACC(adv)	ACC(avg)
Clean	86.57	2.11	44.34
PGD-AT(eps=16/255)	21.83	99.89	60.86
PGD-AT(eps=8/255)	79.27	100.0	89.64
PGD-AWP(eps=16/255)	23.50	100.0	61.75
PGD-AWP(eps=8/255)	24.89	99.81	62.35
Ours	86.10	95.90	91.00

Table 4. The AUC of the baseline systems and the proposed framework against PGD on CASIA-SURF 3DMask.

Model	Method	AUC(%)
Depthnet	PGD-AT(eps=16/255)	73.21
	PGD-AT(eps=8/255)	78.34
	PGD-AWP(eps=16/255)	68.00
	PGD-AWP(eps=8/255)	77.22
	Ours	99.12
CMFL	PGD-AT(eps=16/255)	75.19
	PGD-AT(eps=8/255)	80.63
	PGD-AWP(eps=16/255)	72.71
	PGD-AWP(eps=8/255)	75.50
	Ours	90.94

network away from the clean examples, so the accuracy on the clean examples dramatically reduces. Our AdvFAS not only performs well on clean examples but also has higher accuracy on adversarial examples comparable to the above methods.

AdvFAS vs. Patch Attack. Patch attack is different from a slight noise perturbation adversarial attacks such as PGD, C&W, DeepFool and AutoAttack. The adversarial examples perturbed by patch attack have a specific shape and are much easier to implement in the physical world. In Fig. 3, we show some demos of patch attacks.

We conduct similar experiments in the configuration for patch attacks. The result is shown in Tab. 7 (We also try to test the methods on MI-FGSM and DI-FGSM adversarial attacks in Tab. 5). According to the experimental results, when training with the clean examples, although it has excellent accuracy on the clean examples, the accuracy on face images with patch attack is only about 14% on average. Furthermore, different ad-

Table 5. The performance of the baseline systems and the proposed framework against other adversarial attacks (MI-FGSM and DI-FGSM) on CASIA-SURF 3DMask. And the performance is tested on Depthnet.

Method	Depthnet		
	ACC(w/o adv)	ACC(adv)	ACC(avg)
MI-FGSM-AT	68.22	99.24	83.73
Ours	85.15	93.59	89.37
DI-FGSM-AT	71.18	98.74	84.96
Ours	94.39	87.64	91.02

Table 6. Performance of the baseline systems and the proposed framework against PGD on WMCA. The performance is tested on FAS-wrapper and Patchnet.

Method	FAS-wrapper			Patchnet		
	ACC(w/o adv)	ACC(adv)	ACC(avg)	ACC(w/o adv)	ACC(adv)	ACC(avg)
Clean	92.31	2.36	47.34	91.64	4.54	48.09
PGD-AT(eps=16/255)	52.51	96.18	74.35	53.68	98.39	76.04
PGD-AT(eps=8/255)	73.83	99.04	86.44	74.16	97.46	85.81
PGD-AWP(eps=16/255)	51.38	98.36	74.87	58.39	98.78	78.59
PGD-AWP(eps=8/255)	72.34	96.39	84.37	73.81	98.56	86.19
Ours	87.57	94.17	90.97	88.13	95.18	91.66

versarial training strategies such as patch-AT and patch-AWP can recognize adversarial examples with excellent accuracy, but the accuracy of the clean examples dramatically reduce. Our method significantly improves the metric for detecting adversarial examples while maintaining high performance on clean examples.

On CASIA-SURF 3DMask. To investigate the generality of the proposed framework, we compare with baselines on the second dataset, namely CASIA-SURF 3DMask. We adopt Depthnet as the basic detector, and design experiments to compare AdvFAS with the baseline method, as shown in Tab. 8. Both the ACC(w/o adv) and ACC(avg) of the proposed framework provide the best performance compared to the baseline methods. In fact, the ACC(adv) of our framework is close to 100%.

We attribute the excellent performance of AdvFAS to the coupled relationship between adversarial detection and face anti-spoofing and the training strategy. At training time, the coupled relationship, which can provably distinguish wrongly detected face images from correctly detected ones, can greatly improve the performance of detecting adversarial examples. Our training strategy and the two-head structure bring a small modification to the conventional detector. Therefore, the performance of clean examples fluctuates in a small range. More-

Table 7. Performance of the baseline systems and the proposed framework against patch attack on WMCA. The performance is tested on three models: Depthnet, Resnet18, and Resnet50. Note that only color channels are used on WMCA.

Method	Depthnet			Resnet18			Resnet50		
	ACC(w/o adv)	ACC(adv)	ACC(avg)	ACC(w/o adv)	ACC(adv)	ACC(avg)	ACC(w/o adv)	ACC(adv)	ACC(avg)
Clean	91.10	3.90	47.93	87.58	10.26	51.07	89.90	28.91	58.74
patch-AT(eps=255/255)	21.04	99.99	60.52	21.80	99.98	60.89	20.94	99.93	60.44
patch-AWP(eps=255/255)	20.77	99.83	60.30	20.87	99.94	60.41	21.90	100.0	60.95
patch-AT(eps=125/255)	30.97	99.98	65.48	21.32	99.85	60.59	79.27	100.0	89.64
patch-AWP(eps=125/255)	79.17	100.0	89.58	26.90	98.70	62.80	24.57	100.0	62.28
Ours	92.16	74.78	83.47	93.31	90.04	91.68	89.01	87.8	88.41

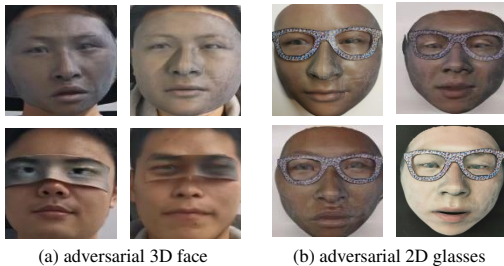


Fig. 4. Examples of test data in real-world scenarios; a) adversarial 3D face crafted for a face recognition system, b) adversarial 2D glasses crafted for a face anti-spoofing system.

Table 8. Performance of the baseline systems and the proposed framework against PGD on CASIA-SURF 3DMask.

Method	Depthnet		
	ACC(w/o adv)	ACC(adv)	ACC(avg)
Clean	99.59	31.30	65.45
PGD-AT(eps=16/255)	31.88	99.71	65.80
PGD-AT(eps=8/255)	68.45	100.0	84.23
PGD-AWP(eps=16/255)	31.40	99.46	65.43
PGD-AWP(eps=8/255)	31.44	100.0	65.72
Ours	99.75	99.88	99.82

over, because all wrongly detected examples are corrected (not just the adversarial examples), the accuracy of clean examples will also improve if the corrector is well optimized. The experimental results of AdvFAS on different adversarial attacks, two publicly available datasets, and widely used backbones are similar. Therefore, our proposed method is efficient in improving the robustness of face anti-spoofing and is compatible with various face anti-spoofing methods.

4.4. In Real-world Scenarios

In this section, we apply our framework to detect adversarial examples in real-world scenarios, as illustrated in Fig. 4. We craft adversarial examples for a face recognition system ArcFace(Deng et al., 2019) and a face anti-spoofing system, respectively, to validate the effectiveness of our framework against adversarial attacks in real-world scenarios.

For the Face Recognition System. Adversarial 3D masks and adversarial 3D patches are crafted to fool face recognition systems. The adversarial 3D patches are crafted through (Yang et al., 2022), which simulates the complex transformations of faces in the physical world via 3D-face modeling. We employ

Table 9. Performance in real-world scenarios

Method	Depthnet			
	ACC(w/o adv)	ACC(adv 3D face)	ACC(adv 2D glasses)	ACC(avg)
Clean	85.96	93.21	20.37	66.51
Patch-AT(eps=16/255)	8.70	92.55	89.34	63.53
Ours	85.08	78.09	88.48	83.58

some volunteers and they are required to wear the adversarial 3D face to record face videos for about 10 seconds. Then, we extract one frame out of every ten frames of each video. Finally, we adopt MTCNN to get 1555 face images as the input images.

For the Face Anti-Spoofing System. We conduct a similar experimental configuration of Sec. 4.3 for patch attack. First, we use patch attacks to generate adversarial 2D glasses for the CMFL. Then, the adversarial examples are printed and cropped to the adversarial 2D glasses. Next, the adversarial 2D glasses are put on the 3D mask to record videos, extract frames, and crop to face images. Finally, the cropped face images are used as the input images of our proposed framework.

The experimental results are shown in Tab. 9. Overall, our proposed framework outperforms the baseline methods. Although, due to the influence of lighting, position, and background, the proposed framework and baseline seem to have a performance gap compared to the results in the digital world. These experimental results show that the proposed framework still detects adversarial examples successfully in real-world scenarios. Furthermore, the results on the adversarial 3D face show that the face anti-spoofing systems have a certain defense against adversarial examples that can fool the face recognition systems.

4.5. Performance Against Adaptive Attacks

We design adaptive attacks to simultaneously evade the detector and corrector. Fig. 5 shows the performance of the proposed framework under adaptive adversarial attacks on WMCA. We explore four different adaptive objectives, including $\mathcal{L}_{spooof} + \eta \cdot \mathcal{L}_{ens}$, $\mathcal{L}_{spooof} + \eta \cdot \mathcal{L}_{cor}$, $\mathcal{L}_{det} + \eta \cdot \mathcal{L}_{ens}$, and $\mathcal{L}_{det} + \eta \cdot \mathcal{L}_{cor}$, where \mathcal{L}_{det} and \mathcal{L}_{cor} is used to directly optimize the spoofing score and correction score respectively. Test Accuracy in each sub-graph represents the detection accuracy, and the horizontal axis represents the value of the coefficient η of \mathcal{L}_{ens} . ACC(adv) is the test accuracy on adversarial examples crafted on WMCA, and ACC(avg) represents the average test accuracy on clean and adversarial examples. When \mathcal{L}_{spooof} and \mathcal{L}_{ens} , or \mathcal{L}_{spooof} and \mathcal{L}_{cor} are combined as the adaptive attack objective, although ACC(adv) and ACC(avg) decrease at first,

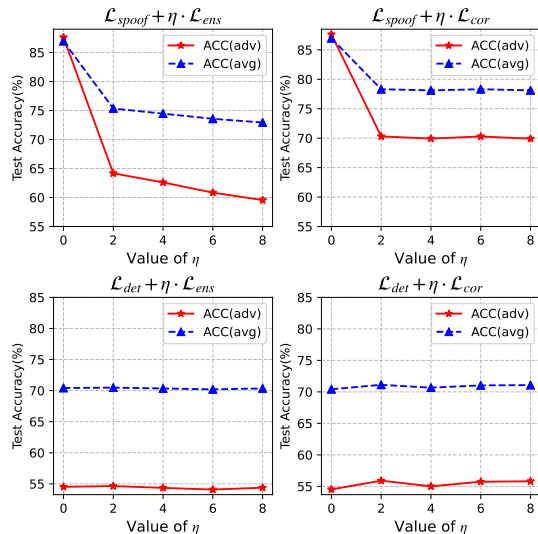


Fig. 5. Performances under adaptive attacks on WMCA. We design four adaptive objectives to evade both the detector and corrector.

the latter trend tends to stabilize with the increase of η . When we combined \mathcal{L}_{det} and \mathcal{L}_{ens} , or \mathcal{L}_{det} and \mathcal{L}_{cor} , even though η is increasing, the values of ACC(adv) and ACC(avg) are relatively stable.

Although there is some decrease in the ACC(adv) and ACC(avg), the ACC(avg) can still reach 70% or more and maintain high performance in detecting clean examples, which means the proposed framework still significantly outperforms baselines. This can be attributed to the coupled mechanism. Specially, when adaptive attacks simultaneously evade the detector and corrector, the accuracy on clean and adversarial examples does not decrease significantly because of the coupled mechanism.

5. Conclusion

In this paper, we first explore the coupled relationship between face anti-spoofing and adversarial detection and then propose a novel face anti-spoofing framework (AdvFAS) against adversarial examples. The effectiveness of the coupled relationship in detecting adversarial examples is proved from both theoretical and practical aspects. By introducing two coupled scores to distinguish incorrectly detected face images from correctly detected ones, our framework significantly improves the robustness of face anti-spoofing technology. We conduct extensive experiments on three backbones and a multi-modal method, two publicly available datasets, and different adversarial attacks to validate the effectiveness our framework. Compared to results without our framework, our best result shows that the accuracy on adversarial examples increased by 93.79%. Experimental results demonstrate that our framework is compatible with various face anti-spoofing methods and maintains excellent performance. Finally, we detect real-world adversarial examples by the proposed framework and demonstrate its practical applicability.

Acknowledgement

This work was supported by the NSFC Projects (Nos. 62076147, 62071292, 62172001, 61771303, U19B2034, U1811461, U19A2081), Tsinghua Institute for Guo Qiang, Tsinghua-OPPO Joint Research Center for Future Terminal Technology, and the High Performance Computing Center, Tsinghua University.

References

- Bousnina, N., Zheng, L., Mikram, M., Ghouzali, S., Minaoui, K., 2021. Unraveling robustness of deep face anti-spoofing models against pixel attacks. *Multimedia Tools and Applications* 80, 7229–7246.
- Carlini, N., Wagner, D., 2017. Towards evaluating the robustness of neural networks, in: 2017 IEEE Symposium on Security and Privacy (SP), IEEE. pp. 39–57.
- Carrara, F., Becarelli, R., Caldelli, R., Falchi, F., Amato, G., 2018. Adversarial examples detection in features distance spaces, in: Proceedings of the European conference on computer vision (ECCV) workshops, pp. 0–0.
- Croce, F., Hein, M., 2020. Reliable evaluation of adversarial robustness with an ensemble of diverse parameter-free attacks, in: International conference on machine learning, PMLR. pp. 2206–2216.
- Deb, D., Liu, X., Jain, A.K., 2021. Unified detection of digital and physical face attacks. *arXiv preprint arXiv:2104.02156*.
- Deng, J., Guo, J., Xue, N., Zafeiriou, S., 2019. Arcface: Additive angular margin loss for deep face recognition, in: Proceedings of the IEEE/CVF conference on computer vision and pattern recognition, pp. 4690–4699.
- Feinman, R., Curtin, R.R., Shintre, S., Gardner, A.B., 2017. Detecting adversarial samples from artifacts. *arXiv preprint arXiv:1703.00410*.
- Freitas Pereira, T.d., Anjos, A., Martino, J.M.D., Marcel, S., 2012. Lbp- top based countermeasure against face spoofing attacks, in: Asian Conference on Computer Vision, Springer. pp. 121–132.
- George, A., Marcel, S., 2019. Deep pixel-wise binary supervision for face presentation attack detection, in: 2019 International Conference on Biometrics (ICB), IEEE. pp. 1–8.
- George, A., Marcel, S., 2021a. Cross modal focal loss for rgb-d face anti-spoofing, in: Proceedings of the IEEE/CVF Conference on Computer Vision and Pattern Recognition, pp. 7882–7891.
- George, A., Marcel, S., 2021b. Cross modal focal loss for rgb-d face anti-spoofing, in: Proceedings of the IEEE/CVF Conference on Computer Vision and Pattern Recognition, pp. 7882–7891.
- George, A., Mostafaei, Z., Geissenbuhler, D., Nikisins, O., Anjos, A., Marcel, S., 2019. Biometric face presentation attack detection with multi-channel convolutional neural network. *IEEE Transactions on Information Forensics and Security* 15, 42–55.
- Gong, Z., Wang, W., Ku, W.S., 2017. Adversarial and clean data are not twins. *arXiv preprint arXiv:1704.04960*.
- Grinchuk, O., Parkin, A., Glazistova, E., 2021a. 3d mask presentation attack detection via high resolution face parts, in: Proceedings of the IEEE/CVF International Conference on Computer Vision, pp. 846–853.
- Grinchuk, O., Parkin, A., Glazistova, E., 2021b. 3d mask presentation attack detection via high resolution face parts, in: Proceedings of the IEEE/CVF International Conference on Computer Vision, pp. 846–853.
- Guo, X., Liu, Y., Jain, A., Liu, X., 2022. Multi-domain learning for updating face anti-spoofing models, in: Computer Vision—ECCV 2022: 17th European Conference, Tel Aviv, Israel, October 23–27, 2022, Proceedings, Part XIII, Springer. pp. 230–249.
- He, K., Zhang, X., Ren, S., Sun, J., 2016. Deep residual learning for image recognition, in: Proceedings of the IEEE conference on computer vision and pattern recognition, pp. 770–778.
- Jee, H.K., Jung, S.U., Yoo, J.H., 2006. Liveness detection for embedded face recognition system. *International Journal of Biological and Medical Sciences* 1, 235–238.
- Jia, Y., Zhang, J., Shan, S., 2021a. Dual-branch meta-learning network with distribution alignment for face anti-spoofing. *IEEE Transactions on Information Forensics and Security* 17, 138–151.
- Jia, Y., Zhang, J., Shan, S., 2021b. Dual-branch meta-learning network with distribution alignment for face anti-spoofing. *IEEE Transactions on Information Forensics and Security* 17, 138–151.

- Jia, Y., Zhang, J., Shan, S., Chen, X., 2020. Single-side domain generalization for face anti-spoofing, in: Proceedings of the IEEE/CVF Conference on Computer Vision and Pattern Recognition, pp. 8484–8493.
- Komulainen, J., Hadid, A., Pietikäinen, M., 2013. Context based face anti-spoofing, in: 2013 IEEE Sixth International Conference on Biometrics: Theory, Applications and Systems (BTAS), IEEE. pp. 1–8.
- Li, J.W., 2008. Eye blink detection based on multiple gabor response waves, in: 2008 International Conference on Machine Learning and Cybernetics, IEEE. pp. 2852–2856.
- Li, S., Zhu, X., Feng, G., Zhang, X., Qian, Z., 2021. Diffusing the liveness cues for face anti-spoofing, in: Proceedings of the 29th ACM International Conference on Multimedia, pp. 1636–1644.
- Li, X., Komulainen, J., Zhao, G., Yuen, P.C., Pietikäinen, M., 2016. Generalized face anti-spoofing by detecting pulse from face videos, in: 2016 23rd International Conference on Pattern Recognition (ICPR), IEEE. pp. 4244–4249.
- Liu, A., Zhao, C., Yu, Z., Su, A., Liu, X., Kong, Z., Wan, J., Escalera, S., Escalante, H.J., Lei, Z., et al., 2021. 3d high-fidelity mask face presentation attack detection challenge, in: Proceedings of the IEEE/CVF International Conference on Computer Vision, pp. 814–823.
- Liu, Y., Chen, Y., Dai, W., Li, C., Zou, J., Xiong, H., 2022. Causal intervention for generalizable face anti-spoofing, in: 2022 IEEE International Conference on Multimedia and Expo (ICME), IEEE. pp. 01–06.
- Liu, Y., Jourabloo, A., Liu, X., 2018. Learning deep models for face anti-spoofing: Binary or auxiliary supervision, in: Proceedings of the IEEE conference on computer vision and pattern recognition, pp. 389–398.
- Ma, X., Li, B., Wang, Y., Erfani, S.M., Wijewickrema, S., Schoenebeck, G., Song, D., Houle, M.E., Bailey, J., 2018. Characterizing adversarial subspaces using local intrinsic dimensionality. arXiv preprint arXiv:1801.02613 .
- Madry, A., Makelov, A., Schmidt, L., Tsipras, D., Vladu, A., 2017. Towards deep learning models resistant to adversarial attacks. arXiv preprint arXiv:1706.06083 .
- Metzen, J.H., Genewein, T., Fischer, V., Bischoff, B., 2017. On detecting adversarial perturbations. arXiv preprint arXiv:1702.04267 .
- Ming, Z., Yu, Z., Al-Ghadi, M., Visani, M., Luqman, M.M., Burie, J.C., 2022. Vitranspad: Video transformer using convolution and self-attention for face presentation attack detection, in: 2022 IEEE International Conference on Image Processing (ICIP), IEEE. pp. 4248–4252.
- Moosavi-Dezfooli, S.M., Fawzi, A., Frossard, P., 2016. Deepfool: a simple and accurate method to fool deep neural networks, in: Proceedings of the IEEE conference on computer vision and pattern recognition, pp. 2574–2582.
- Pan, G., Sun, L., Wu, Z., Lao, S., 2007. Eyeblink-based anti-spoofing in face recognition from a generic webcam, in: 2007 IEEE 11th international conference on computer vision, IEEE. pp. 1–8.
- Pang, T., Zhang, H., He, D., Dong, Y., Su, H., Chen, W., Zhu, J., Liu, T.Y., 2022. Two coupled rejection metrics can tell adversarial examples apart, in: Proceedings of the IEEE/CVF Conference on Computer Vision and Pattern Recognition, pp. 15223–15233.
- Patel, K., Han, H., Jain, A.K., 2016. Secure face unlock: Spoof detection on smartphones. IEEE transactions on information forensics and security 11, 2268–2283.
- Shafahi, A., Najibi, M., Ghiasi, M.A., Xu, Z., Dickerson, J., Studer, C., Davis, L.S., Taylor, G., Goldstein, T., 2019. Adversarial training for free! Advances in Neural Information Processing Systems 32.
- Szegedy, C., Zaremba, W., Sutskever, I., Bruna, J., Erhan, D., Goodfellow, I., Fergus, R., 2013. Intriguing properties of neural networks. arXiv preprint arXiv:1312.6199 .
- Tong, L., Chen, Z., Ni, J., Cheng, W., Song, D., Chen, H., Vorobeychik, Y., 2021. Facesecc: A fine-grained robustness evaluation framework for face recognition systems, in: Proceedings of the IEEE/CVF Conference on Computer Vision and Pattern Recognition, pp. 13254–13263.
- Tramer, F., Carlini, N., Brendel, W., Madry, A., 2020. On adaptive attacks to adversarial example defenses. Advances in Neural Information Processing Systems 33, 1633–1645.
- Wang, C.Y., Lu, Y.D., Yang, S.T., Lai, S.H., 2022a. Patchnet: A simple face anti-spoofing framework via fine-grained patch recognition, in: Proceedings of the IEEE/CVF Conference on Computer Vision and Pattern Recognition, pp. 20281–20290.
- Wang, W., Wen, F., Zheng, H., Ying, R., Liu, P., 2022b. Conv-mlp: A convolution and mlp mixed model for multimodal face anti-spoofing. IEEE Transactions on Information Forensics and Security 17, 2284–2297.
- Wang, Z., Wang, Q., Deng, W., Guo, G., 2022c. Learning multi-granularity temporal characteristics for face anti-spoofing. IEEE Transactions on Information Forensics and Security 17, 1254–1269.
- Wiyatno, R., Xu, A., Dia, O., de Berker, A., . Adversarial examples in modern machine learning: A review. arxiv 2019. arXiv preprint arXiv:1911.05268 .
- Wu, D., Xia, S.T., Wang, Y., 2020. Adversarial weight perturbation helps robust generalization. Advances in Neural Information Processing Systems 33, 2958–2969.
- Yang, J., Lei, Z., Li, S.Z., 2014. Learn convolutional neural network for face anti-spoofing. arXiv preprint arXiv:1408.5601 .
- Yang, J., Liu, J., Han, R., Wu, J., 2021a. Generating and restoring private face images for internet of vehicles based on semantic features and adversarial examples. IEEE Transactions on Intelligent Transportation Systems .
- Yang, X., Dong, Y., Pang, T., Su, H., Zhu, J., Chen, Y., Xue, H., 2021b. Towards face encryption by generating adversarial identity masks, in: Proceedings of the IEEE/CVF International Conference on Computer Vision, pp. 3897–3907.
- Yang, X., Dong, Y., Pang, T., Xiao, Z., Su, H., Zhu, J., 2022. Controllable evaluation and generation of physical adversarial patch on face recognition. arXiv e-prints , arXiv-2203.
- Yang, X., Luo, W., Bao, L., Gao, Y., Gong, D., Zheng, S., Li, Z., Liu, W., 2019. Face anti-spoofing: Model matters, so does data, in: Proceedings of the IEEE/CVF Conference on Computer Vision and Pattern Recognition, pp. 3507–3516.
- Yin, B., Wang, W., Yao, T., Guo, J., Kong, Z., Ding, S., Li, J., Liu, C., 2021. Adv-makeup: A new imperceptible and transferable attack on face recognition. arXiv preprint arXiv:2105.03162 .
- Yu, Z., Qin, Y., Li, X., Zhao, C., Lei, Z., Zhao, G., 2022. Deep learning for face anti-spoofing: A survey. IEEE Transactions on Pattern Analysis and Machine Intelligence .
- Yu, Z., Qin, Y., Zhao, H., Li, X., Zhao, G., 2021. Dual-cross central difference network for face anti-spoofing. arXiv preprint arXiv:2105.01290 .
- Yu, Z., Wan, J., Qin, Y., Li, X., Li, S.Z., Zhao, G., 2020. Nas-fas: Static-dynamic central difference network search for face anti-spoofing. IEEE transactions on pattern analysis and machine intelligence 43, 3005–3023.
- Zhang, C., Ye, Z., Wang, Y., Yang, Z., 2018. Detecting adversarial perturbations with saliency, in: 2018 IEEE 3rd International Conference on Signal and Image Processing (ICSIP), IEEE. pp. 271–275.
- Zhang, H., Yu, Y., Jiao, J., Xing, E., El Ghaoui, L., Jordan, M., 2019. Theoretically principled trade-off between robustness and accuracy, in: International conference on machine learning, PMLR. pp. 7472–7482.
- Zhang, K., Zhang, Z., Li, Z., Qiao, Y., 2016. Joint face detection and alignment using multitask cascaded convolutional networks. IEEE signal processing letters 23, 1499–1503.
- Zhang, W., Liu, H., Ramachandra, R., Liu, F., Shen, L., Busch, C., 2021. Face presentation attack detection using taskonomy feature. arXiv preprint arXiv:2111.11046 .